Lasers in Medical Science (2023) 38:87
https://doi.org/10.1007/s10103-023-03746-w

ORIGINAL ARTICLE

Single intraoperative infrared laser optimized bone repair in rat femoral osteotomies with experimentally induced osteoporosis

Tárik Ocon Braga Polo[1] · João Matheus Fonseca-Santos[1] · Gustavo Antonio Correa Momesso[1,2] · William Phillip Pereira da Silva[1] · Stefany Barbosa[1] · Anderson Maikon de Souza Santos[1] · Mirela Caroline Silva[1] · Valdir Gouveia Garcia[3] · Letícia Helena Theodoro[3] · Leonardo P. Faverani[3]

Received: 2 March 2022 / Accepted: 6 March 2023 / Published online: 20 March 2023

Abstract

This study aimed to evaluate the effect of infrared laser (IRL) on bone repair in ovariectomized rats subjected to femoral osteotomies. Of 32 rats, half underwent bilateral ovariectomy (OVX) and the other half underwent sham ovariectomy (SHAM). A period of 3 months was defined to observe the presence of osteoporosis. The rats were subjected to osteotomies in the femurs and then fixed with a miniplate and 1.5-mm system screws. Thereafter, half of the rats from both SHAM and OVX groups were not irradiated, and the other half were irradiated by IRL using the following parameters: wavelength, 808 nm; power, 100 mW; 60 s for each point; 6 J/point; and a total of 5 points of bone gap. All animals were euthanized 60 days after surgery. The femur gap was scanned using micro-computed tomography (micro-CT). The samples were then examined under a confocal laser microscope to determine the amounts of calcein and alizarin red. The slides were stained with alizarin red and Stevenel's blue for histometric analysis. In the micro-CT analysis, the OVX groups had the lowest bone volume ($P < 0.05$). When the laser was applied to the OVX groups, bone turnover increased ($P < 0.05$). New bone formation (NBF) was comparable between SHAM and OVX/IR ($P > 0.05$) groups; however, it was less in the OVX groups ($P < 0.05$). In conclusion, the results encourage the use of IRL intraoperatively as it optimizes bone repair, mainly in animals with low bone mineral density.

Keywords Osteoporosis · Bone regeneration · Fracture fixation internal · Laser therapy

Introduction

Osteoporosis is a systemic condition that occurs mostly in women after menopause but also in men after andropause, and it is linked to hormonal deficiency in both cases. It can facilitate the occurrence of fractures and debilitating complications [1]. Experimental studies have simulated the induction of bone mass reduction through ovariectomy in female rats, characterized by experimental osteoporosis [2–4].

During the restructuring of fractured bone tissue, osteoporosis causes a reduction in bone tissue quantity and microstructural characteristics, which may delay the chronological phases of fracture repair and destabilize the repair gap between fractured stumps. Instead of producing bone with a good degree of maturation, an interposition of fibrous connective tissue, called pseudarthrosis, is formed, leading to complications such as infections and treatment failure [5].

Photobiomodulation (PBM) therapy is a widely studied concept for optimizing bone repair in critical situations. PBM therapy involves the application of monochromatic light with a low energy density that promotes non-thermal photochemical effects at the cellular level [6, 7]. In vivo and in vitro investigations have shown that PBM therapy can accelerate the repair of bone defects [8]. These results show an increase in osteoblastic activity, vascular neoformation, collagen fiber organization, and mitochondrial alterations [9–11].

Dentistry studies demonstrating the clinical application and effectiveness of PBM in treating fractures remain scarce.

✉ Leonardo P. Faverani
leonardo.faverani@unesp.br

[1] School of Dentistry, São Paulo State University (UNESP), Araçatuba, São Paulo, Brazil

[2] Department of Implantology, University of Santo Amaro, Unisa, São Paulo, SP, Brazil

[3] Diagnosis and Surgery Department, School of Dentistry, São Paulo State University (UNESP), 1193 José Bonifácio Street, Araçatuba, São Paulo 16015-050, Brazil

Moreover, standardized protocols for its intraoperative application have not yet been established [12–15].

Briteño-Vasequez et al. [16] evaluated the effect of infrared laser (IRL) on tibial fractures in rats after 10 applications in the region of fracture fixation during the postoperative period. The rats were irradiated with an arsenic-gallium (GaA) laser using the following parameters: wavelength, 850 nm; power, 100 mW; and energy, 8 J/cm^2 for 64 s. The radiological and histopathological parameters were more superior in the group of animals that underwent IRL irradiation than in those that did not. However, Sella et al. [17] demonstrated that multiple applications (eight applications) did not lead to a higher level of calcification, which the bone repair reached a plateau. The beginning of bone repair showed an acceleration of osteogenesis activity, leading us to thinking of this proposal, using a single dose of IRL.

Therefore, this study aimed to evaluate the effect of a single intraoperative application of IRL on bone repair in femoral osteotomy in osteoporotic female rats. The null hypothesis is that IRL single session treatment cannot influence bone repair in induced osteoporosis.

Methodology

Animals

This study was approved by the Ethics Committee on Animal Experiments (# 00,287–2017, Faculty of Dentistry of Araçatuba, UNESP, Brazil). Overall, 32 female rats (*Rattus albinus*, Wistar) aged 6 months, with body weight ranging from 250 to 300 g throughout the course of the experiment, were studied. The rats were kept in cages (four per cage) in an environment with a stable temperature (22 ± 2 °C) and a controlled light cycle (12 h of light and 12 h of darkness). They were fed solid food and water ad libitum during the entire experiment, except for periods of 8 h before the surgical procedures.

Experimental model

The sample size was determined on the basis of a previous study. The data of mean difference (9.9) and standard deviation (14.41) and test power of 95%, regarding the primary outcome (new bone formation [NBF]), were considered. A sample size of 32 rats was defined, with eight rats/16 femurs per experimental group [18].

The animals were subjected to bilateral ovariectomy to induce osteoporosis due to estrogen deficiency. Sixteen female rats were randomly selected to undergo bilateral ovariectomy (OVX), and the remaining rats ($n = 16$) were subjected to sham ovariectomy (SHAM), i.e., only surgical exposure, and not removal, of the ovaries [19–23]. The rats were sedated with xylazine hydrochloride (Xylazine; Coopers, Brazil, Ltd.) at a dose of 5 mg/kg and ketamine hydrochloride (Ketamine; Fort Dodge, Saúde Animal Ltd.) at a dose of 50 mg/kg. This procedure was performed as previously reported [24–27].

Enzyme immunoassay was used to assess blood samples collected from the rats during euthanasia to determine the difference between OVX and SHAM rats in terms of plasma concentration of estrogen.

Femoral osteotomy

The rats underwent osteotomy 90 days after osteoporosis induction [4]. The rats were sedated again with a combination of ketamine and xylazine (with the same doses used for the ovariectomy procedure). Considering that a low-intensity IRL was used, the allocation was determined randomly by drawing lots. Subsequently, using a number 15 blade (Feather Industries Ltd., Tokyo, Japan), a 4-cm-long incision was made in the lateral portion of the femur. A circular saw of 2-mm thickness was used, and the osteotomy was performed in the epiphyseal metaphysis [27–29]. A 1.5-mm titanium plate with four holes and corresponding bicortical screws was used for osteotomy fixation (Engimplan Engenharia de Implantes, Rio Claro, SP, Brazil). During the entire procedure, including the osteotomy and perforation with surgical drills, the regions were copiously irrigated with physiological saline solution to avoid heating the bone tissue and thus negatively influencing bone repair. The tissues were then sutured.

Four experimental groups were divided according to bone quality and IRL application: SHAM (femurs subjected to sham surgery without PBM); SHAM/IR (femurs subjected to sham surgery with PBM); OVX (osteoporotic femurs without PBM); and OVX/IR (osteoporotic femurs with PBM) (Fig. 1).

PBM through the application of IRL

For SHAM/IR and OVX/IR, after fixation and osteotomy, the bone gap areas were irradiated with a low-intensity GaAs diode laser (DMC Equipamentos, São Paulo, Brazil). The protocol was as follows: wavelength, 808 nm; power, 100 mW; spot size, 0.0283 cm^2; energy density, 212 J/cm^2; power intensity, 3.53 W/cm^2; and continuous mode for 60 s at each point, 6 J/point and a total five application points in all areas of the bone gap, totalizing 30 J of energy on each femur [18]. After irradiation, all anatomical tissue layers were sutured (Fig. 2).

Both animals' femurs were operated on, in which the same treatment was performed to avoid bias in terms of PBM and no PBM application for SHAM and OVX groups.

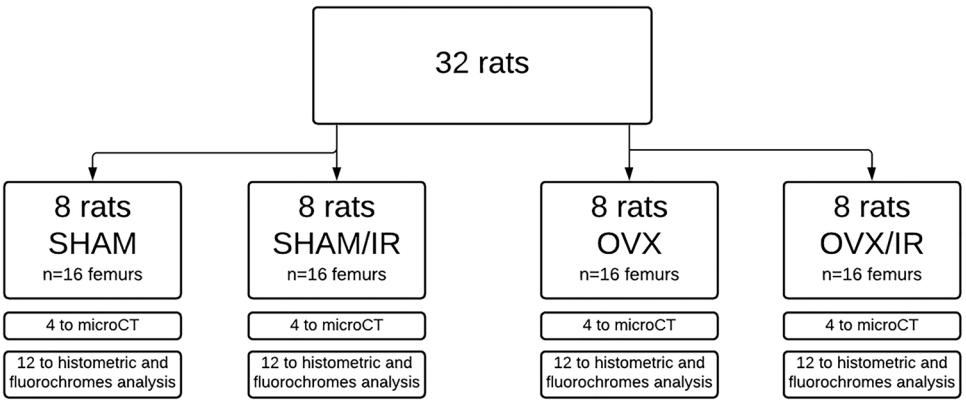

Fig. 1 A representative flowchart of the experimental groups, according to the systemic condition and use of photobiomodulation

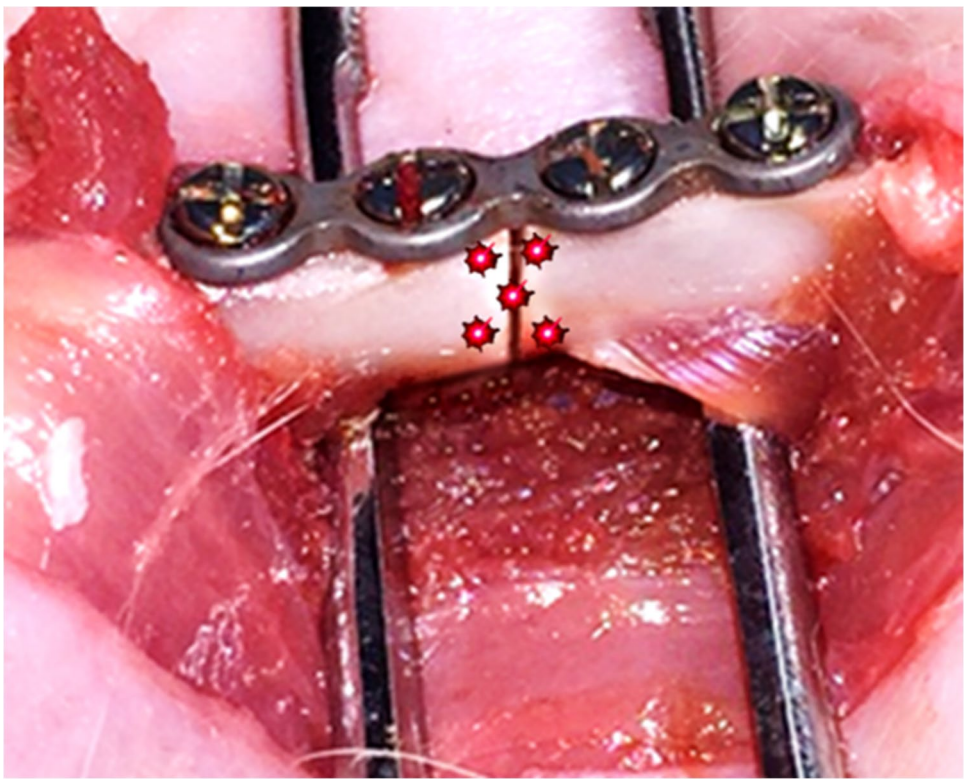

Fig. 2 Five laser application points in the proximal, central, and distal portions of the femoral fracture region

Lab processing

Sixty days after the last surgery, all the animals were euthanized with an anesthetic overdose (intraperitoneal sodium thiopental, 150 mg/kg). The femurs were stored in 10% formalin for 48 h after removal. The femurs had been completely removed, with at least 4 mm remaining on each side of the bone stumps (bone repair gap). The samples were stored in 70% alcohol and subjected to microtomography. Shortly after that, the femurs were processed for cutting and grinding in the Exakt system for calcified tissues, thus making it possible to obtain 100-µm-thick slices (Exakt Cutting System, Apparatebau GmbH, Hamburg, Germany). The area of interest for evaluation was the entire extent of the repair gap caused by the osteotomy. These laboratory procedures have been reported in our previous in vivo study [23].

Micro-computed tomography

The samples of 5-µm thickness (50 kV and 500 µ) were scanned using a SkyScan micro-computed tomography (micro-CT) scanner (SkyScan 1176 Bruker MicroCT, Aartselaar, Belgium, 2003), with a copper and aluminum filter and a rotation step of 0.3 mm. The images taken by X-ray projection on the samples were stored and reconstructed using the NRecon software (SkyScan, 2011; version 1.6.6.0). This software helped determine which parts of the samples were of interest.

Using the Data Viewer software (SkyScan, version 1.4.4, 64-bit), the images were reconstructed to adapt to the standard positioning for all samples, which can be observed in three planes (transverse, longitudinal, and sagittal). Then, using the CTAnalyser software (CTAn; 2003–11SkyScan, 2012 Bruker MicroCT, version 1.12.4.0), the region of interest (ROI) was delimited by the repair gap created by the osteotomy between the two femoral stumps. The CTAn software analyzes and measures the image according to the grayscale threshold. The threshold used in the analysis was 25–90 shades of gray; thus, the volume of the bone formed in the ROI could be obtained by referring to the NBF. Parameters related to the amount of bone tissue—BV/TV = percentage of bone volume and Po.Tot = percentage of total porosity—and bone quality—Tb.Th = thickness of the bone trabeculae, Tb.SP = separation of bone trabeculae, and Tb.N = number of trabeculae—were assessed [30].

Scanning using confocal laser microscopy for analysis of bone dynamics in repair

On the 14th and 42nd postoperative days, the fluorochrome calcein and alizarin red, respectively, were administered intramuscularly at a dose of 20 mg/kg of animal weight, allowing analysis under confocal microscopy. After processing the slides in an automatic cutting system (Exakt Cutting System, Apparatebau GmbH, Hamburg, Germany), with sections of approximately 100 µm, they were analyzed using a confocal laser microscope (Leica CTR 4000 CS SPE Leica Microsystems, Heidelberg, Germany). The slides were scanned in the z-stack mode and observed from the onset of the fluorescence. The size of the images was 1×1 mm^2, corresponding to optical sections of 512×512 pixels. BP 530/30 nm and 590 LP filters were used, in combination with 488/568 nm "double dichroic" activation. The photomultiplier was set to filters 534 (blue filter) and 357 (green filter), which allowed calcein and alizarin, respectively, to be visualized. After reconstruction, all images were exported to ImageJ software (Processing Software and Image Analysis, Ontario, Canada) and standardized with the "color threshold" tool, with the marking area determined in µm^2 using the "measure" tool [23, 27].

The femur (ROI: repair gap) should have two overlays of fluorochromes (calcein and alizarin). Each overlay represents calcium precipitated in each period, thus indicating the conversion of old bone to new bone. These images were assessed in the ImageJ software using the color threshold tool. Each image was standardized according to hue, saturation, and brightness to reveal the fluorochromes. First, calcein (green color) was highlighted, and the measure tool was used to provide the area in µm^2. The same procedure was performed for alizarin (red color) to obtain data on the dynamics of the reparative bone.

Bone turnover is represented by the difference between the old bone (green) and new bone (red). From the superimposed images (red/green), using the "freehand" tool in the ImageJ software, the area in pixels^2 was measured for bone mineral measurement. On this basis, we infer that the different colors represent the bones formed in different periods. Bone tissue dynamics are defined by bone turnover, which is observed through bone renewal and is represented by red fluorochromes. The higher the intensity of red fluorescence, the greater the formation of new bone; in contrast, green fluorescence represents old bone.

Histometric analysis

After analysis under a confocal microscope, the slides were washed with deionized water and stained with alizarin red and Stevenel's blue. Photomicrographs were obtained using an optical microscope with an objective lens of × 25. The same ROI (bone repair gap) was measured to analyze the area of new bone formation (NBF). Thus, after photomicrography of the histological slides, they were assessed using ImageJ, where, using the free hands tool, the NBF area was measured in µm^2. The evaluators were blinded to the identity of rat groups, and the groups were named a, b, c, or d.

Statistical analysis

All quantitative data obtained in this study (NBF; area of fluorochromes: calcein/alizarin) and micro-CT (BV/TV, Tb.Th, Tb.Sp, and Tb.N) findings were statistically analyzed. The difference between the experimental groups regarding IRL performance (with or without IRL application) was also addressed. Data were first subjected to the Shapiro–Wilk normality test, which revealed homogeneous data interactions ($P > 0.05$). Experiments were performed separately in the SHAM and OVX groups. Therefore, a two-way analysis of variance (ANOVA) test was applied to assess the dynamism of bone repair (calcein and alizarin deposition). For the analyses of NBF areas and micro-CT images, a one-way ANOVA test was applied. Tukey's post hoc test was performed for each parameter when the interactions showed $P < 0.05$. The statistical program SigmaPlot 12.0 was used (Exakt Graphs and Data Analysis, San Jose, CA, USA).

Results

Plasma estradiol concentration

The results obtained through the immunoassay for estrogen by the ELISA test showed a significant decrease in plasma estradiol in ovariectomized animals (7.3 ± 1.4 ng/mL) compared to SHAM animals (52.4 ± 18.1 ng/mL) ($P < 0.001$, t-test).

Micro-Ct

In the three-dimensional reconstructions, the OVX groups maintained a gap between the stumps of bone repair, indicating an unconsolidated bone gap. OVX IR showed a hyperdensity closing the bone gap and in the medullary space forming the bone callosity. For the BV/TV data, the OVX groups showed lower values than the SHAM groups ($P < 0.05$). For Tb.N, the IR groups presented better results than those without irradiation ($P < 0.05$). For Tb.Sp, compared with the other groups, the OVX groups presented the highest values ($P < 0.05$). For Po.Tot, SHAM groups showed more increased areas than OVX groups ($P < 0.05$), and compared with the non-irradiated groups, IR groups also presented a favorable difference ($P < 0.05$) (Tables 1 and 2; Fig. 3).

Analysis of bone dynamics in repair

The analysis of calcein and alizarin precipitation area showed a lower deposition of both fluorochromes in the OVX groups (green: 3.07 pixels/cm^2; red: 1.35 pixels/cm^2) ($P < 0.05$) than in the SHAM (green: 6.67 pixel/cm^2; red: 5.11 pixel/cm^2), SHAM/IR (green: 8.33 pixel/cm^2; red: 4.96 pixel/cm^2), and OVX/IR (green: 5.19 pixels/cm^2; red: 3.57 pixels/cm^2) groups, indicating poor bone deposition and bone turnover. An important emphasis was given to comparing OVX with OVX/IR, where the application of laser in a single section generated greater precipitation of calcein and alizarin, demonstrating higher values of bone tissue renewal ($P < 0.05$) (Table 3; Fig. 4).

Table 1 Quantitative results of BV.TV and Po.Tot, evidencing the superiority of the SHAM groups, compared to the OVX, in view of the osteoporotic condition. Lower case letters—a—indicate a statistical difference for the groups with upper case letters—A, $P < 0.05$

Group	BV.TV (%)	SD	Po.Tot (%)	SD
SHAM	81.662^A	5.679	69.092^A	7.580
SHAM/IR	63.248^A	1.530	62.229^A	6.969
OVX	52.977^a	1.289	40.253^a	1.302
OVX/IR	58.275^a	1.271	49.528^a	1.185
P-value	$P < 0.05$		$P < 0.05$	

New bone formation

Qualitative analysis clearly showed a good bone repair appearance in healthy animals (SHAM), with a large amount of bone tissue found mostly in the femoral gap and only a small amount in the adipose tissue. In contrast, the OVX groups showed more areas of negatively marked images characteristic of vacuoles of the adipose architecture. Regarding IR, it was possible to identify positive characteristics in the SHAM groups and more significantly in the OVX groups concerning the pattern of bone neoformation and the amount of NBF (Table 4; Fig. 5). In short, NBF in the OVX/IR groups was higher than that in OVX without IR application ($P < 0.05$) and was similar to that in the SHAM groups ($P > 0.05$; OVX/IR = SHAM).

Discussion

The main objective of this preclinical study was to evaluate the influence of a single intraoperative IRL application on the repair of femoral osteotomies in animals characterized by low bone mineral density (BMD). We noticed that the PBM therapy with IRL provided a noticeable improvement during repair, with a larger area of bone neoformation in the repair gap than in the groups that did not receive PBM therapy.

To characterize the experimental model of low BMD, ovariectomy was performed to remove the bilateral ovaries. As per FDA guidelines, we expected that osteoporosis would be established in the animals 90 days after the ovariectomy [31]. In this study, the OVX group showed a significant decrease in plasma estradiol compared to SHAM animals. Although no densitometry measurements were taken in this investigation, severe hypoestrogenism is widely known to cause BMD loss [2, 32]. Furthermore, all parameters from micro-CT related to bone volume and bone quality showed a severe decrease in values for the OVX groups, corroborating this assertion.

In addition, this model was adopted because of the deficient characteristics caused by osteoporosis, such as loss of BMD and, consequently, increased bone fragility which considerably interferes with bone remodeling and leads to delayed tissue repair [2, 3]. Preclinical studies have shown that ovariectomized animals subjected to femoral fracture

Table 2 The quantitative results of Tb.N, Tb.SP, and Tb.Th. Lower case letters—a—indicate a statistical difference for the groups with upper case letters—A, $P < 0.05$

Group	Tb.N (1/mm)	SD	Tb.Sp (mm)	SD	Tb.Th (mm)	SD
SHAM	2.356^A	3.711	1.327	5.876	0.282	0.06
SHAM/IR	2.887^A	7.695	1.311	4.676	0.266	0.10
OVX	1.787^a	1.576	1.339	3.919	0.232	0.06
OVX/IR	2.505^A	3.614	1.285	8.062	0.357	0.05
P-value	$P < 0.05$		$P > 0.05$		$P > 0.05$	

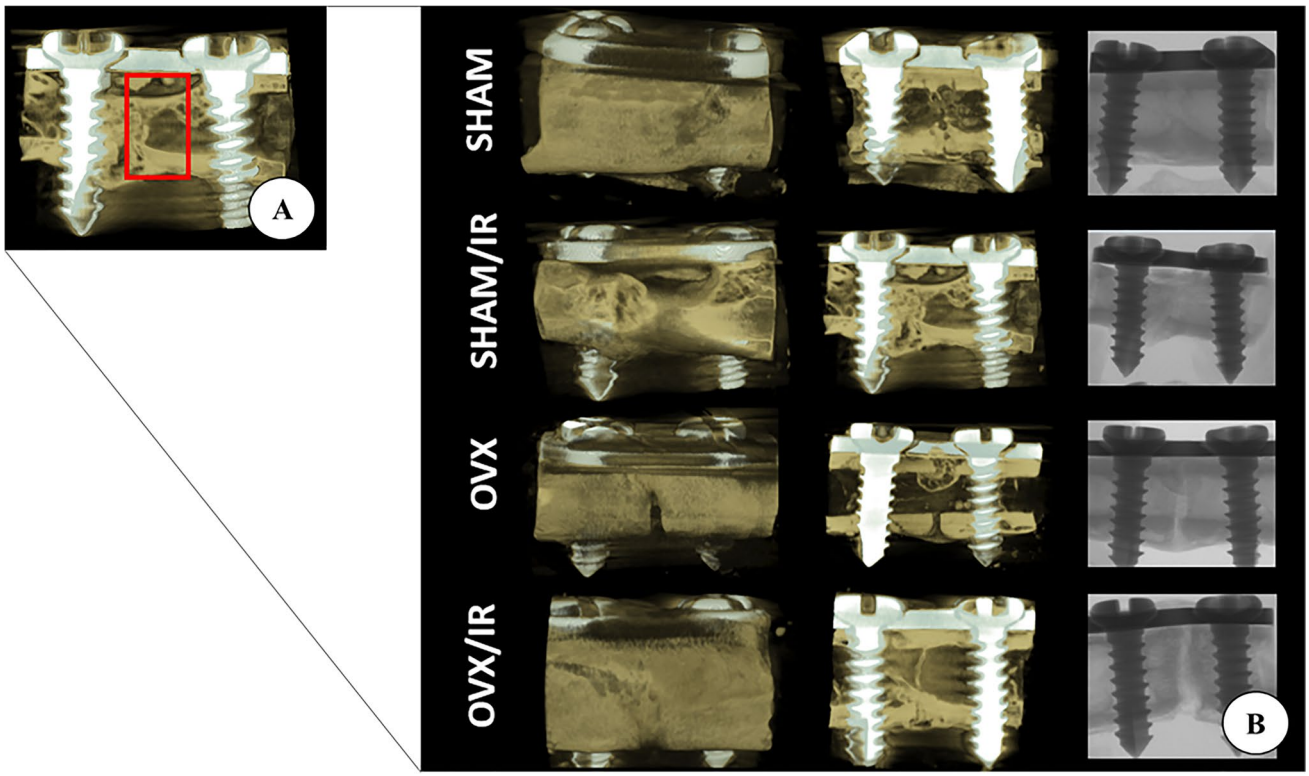

Fig. 3 **A** Demarcation of the analyzed ROI. **B** Three-dimensional comparison of the experimental groups

Table 3 Quantitative results of the dynamics of calcein green and alizarin red. The results of the measurement of bone dynamics marked by fluorochromes in the gap and cortical bone near the plate showed a lower result for the OVX groups, with a significant difference compared to the other groups both in calcein and alizarin red staining. Lower case letters—a—indicate a statistical difference for the groups with upper case letters—*A*, $P < 0.05$

Group	Green (pixel/cm^2)	SD	Red (pixel/cm^2)	SD
SHAM	6.67^A	4.21	5.11^A	1.60
SHAM/IR	8.33^A	1.59	4.96^A	2.12
OVX	3.07^a	1.85	1.35^a	1.14
OVX/IR	5.19^A	0.60	3.57^A	0.43
P-value	$P < 0.05$		$P < 0.05$	

simulation and fixed with conventional titanium plates present with more delayed tissue repair than healthy animals do [32, 33]. A study by Campenfeldt et al. [34] showed that patients with low BMD had more failures in the fixation of femoral fractures than those with adequate BMD.

The optimization of the repair was verified in the IR groups through the application of IRL treatment at the time of surgical bone fixation, corroborating in part the results of Briteño-Vasequez et al. [16], which also showed improved radiological and histological outcomes for groups that received PBM therapy, even in rats with no bone metabolism alteration. On comparing SHAM and OVX, our results showed that the application of PBM therapy in OVX femoral osteotomies optimized bone repair more. Previous studies have shown that PBM is active and acts on lesioned cells when improvements in cell response are needed [35, 36].

The improvement in bone repair in the IR groups is highlighted by the sum of the results obtained from the histometric and micro-CT analyses, representing a greater number of areas of NBF as well as superior quality of the microarchitecture. The bone volume of the OVX groups was lesser than that of the SHAM groups, which was expected because of the low BMD caused by osteoporosis. The OVX/IR group had the same number of bone trabeculae as the SHAM group, but with more bone thickness. This could be because OVX/IR helped the group recover from osteoporosis.

A study by Shakouri et al. [35] showed that PBM therapy with IRL (780 nm) in animals may facilitate fracture healing in the early stages but with weak biomechanical properties. Therefore, they recommended the use of this type of laser therapy for humans only in cases of bone malformation, such as unjointed fractures. The use of any adjuvant therapy, such as PBM therapy, for fractures is not recommended as an isolated treatment. Adequate fixation of the fracture is necessary, and often, some drug therapy is also indicated [37].

According to the evaluated confocal microscopy parameters, we observed that healthy animals (SHAM) presented positive

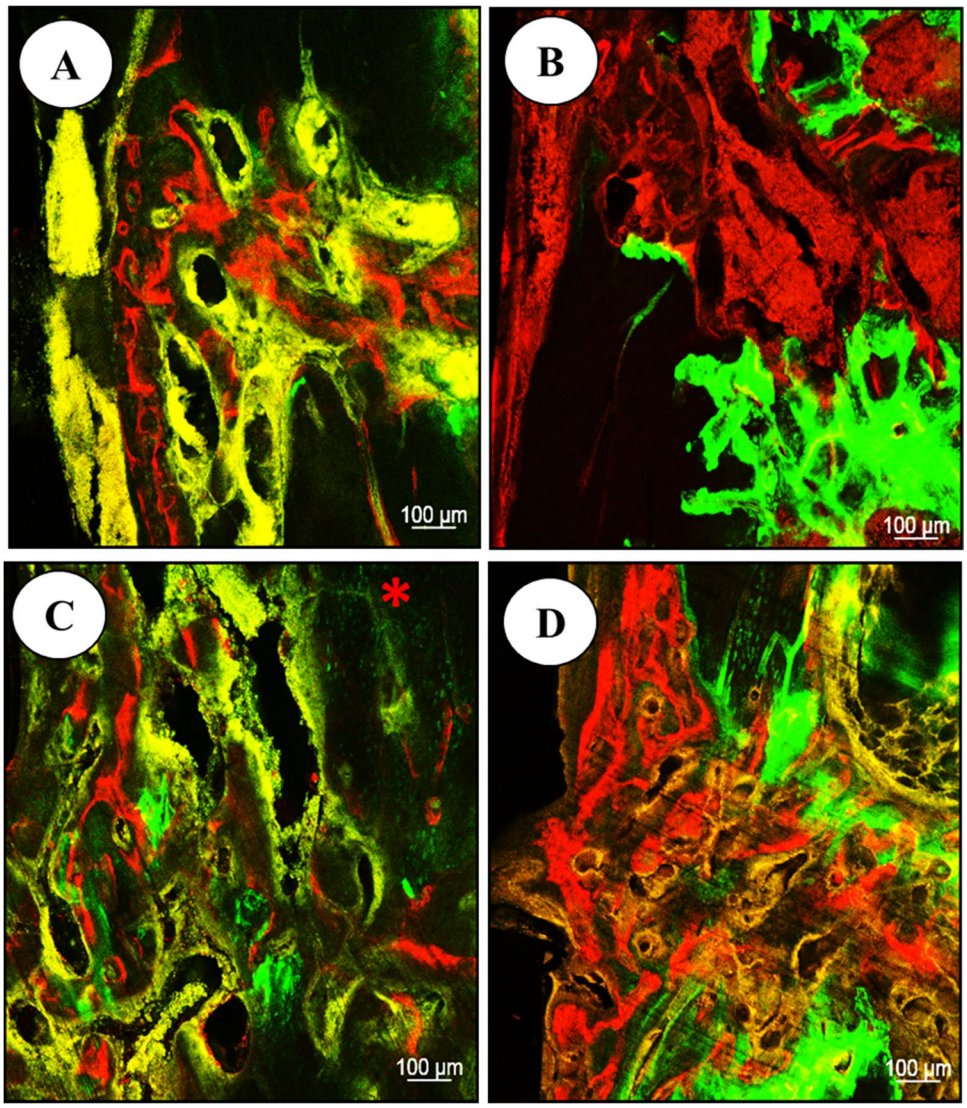

Fig. 4 **A**–**D** Qualitative results of the SHAM, SHAM/IR, OVX, and OVX/IR groups, respectively. *The OVX group where the highest calcein green staining is observed, demarcating the largest area of old bone. Original magnification = × 10. Scale bar = 100 µm

Table 4 Quantitative data referring to the area of new bone formed (NBF); the measurement of the area of NBF in the gap and the cortical area close to the plate showed a lower result for the OVX group with a significant difference compared to the OVX/IR group and SHAM groups ($P < 0.05$). Lower case letters—a—indicate a statistical difference for the groups with upper case letters—*A*, $P < 0.05$

Group	NBF (%)	SD
SHAM	53,90^{A}	10.96
SHAM/IR	49.70^{A}	7.47
OVX	38.70^{a}	10.68
OVX/IR	48.60^{A}	2.69
P-value	$P < 0.05$	

bone repair patterns, regardless of laser application. Regarding the osteoporotic groups (OVX), we noticed that PBM significantly improved the repair pattern. NBF was lower in the OVX groups; however, there was no statistically significant difference between the OVX/IR and SHAM groups. These results show that PBM therapy improves bone repair in animals with low BMD. The notable difference between OVX vs. OVX/IR and SHAM vs. SHAM/IR reinforces the OVX model as a significant critical bone condition related to osteoporosis generated by estrogen suppression after ovariectomy.

The literature suggests that the improvement in bone repair with the use of PBM therapy is due to a modulation of the local inflammatory response induced by chemotaxis, with the recruitment of cells and precursor chemical mediators of tissue repair [38, 39]. In this context, this process occurs physiologically in healthy organisms; however, in deficient organisms, PBM therapy becomes more effective owing to the stimulation and recruitment of bone cells, since the antioxidant effects of PBM promote a favorable microenvironment for the occurrence of bone tissue deposition. This allows the OVX/IR group to present results similar to those of healthy groups [40, 41].

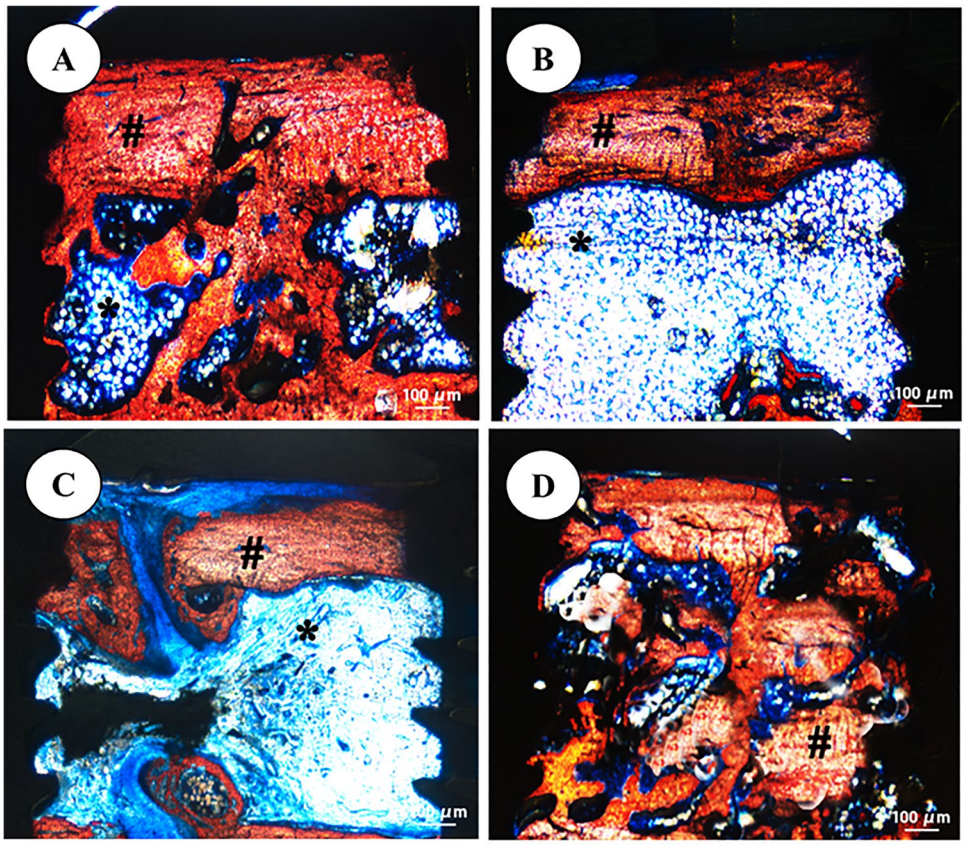

Fig. 5 **A**–**D** Qualitative results from the SHAM, SHAM/IR, OVX, and OVX/IR groups, respectively. A greater deposition of bone tissue in the region of interest is observed in the OVX/IR group (**D**), compared to the OVX (**C**), which also shows the interposition of connective tissue, indicating a delay in the repair. Staining: alizarin red and Stevenel blue. Original magnification = × 10. Scale bar = 100 µm (#bone tissue and *soft tissue)

The effects of PBM therapy have been linked to several factors. Amaroli et al. [42] elucidated through a systematic review that the wavelength used in this study (808 nm) is within a specific IRL range and is capable of effectively photosensitizing bone tissue cells, corroborating the results obtained regarding bone tissue neoformation and dynamics. Furthermore, other parameters associated with lasers, such as energy (Joule = J), power (Watt = W), power density (W/cm^2), irradiation mode (continuous or pulsed), duration, and number of applications, should be considered [43]. In this study, only an intraoperative application was performed. Given that the results were good, we aim to conduct more studies with more applications so as to add to the results and determine the best way to apply PBM therapy.

However, the animals in which osteoporosis was induced (OVX groups) did not receive any systemic treatment for the disease. Therefore, fully reversing the deterioration of bone microarchitecture is impossible, and this is not the objective of PBM therapy; however, PBM therapy has a high potential for cell activation without systemic adverse effects. Clearly, PBM therapy improved the bone repair gap investigated in this study and may be used in association with other protocols to establish a consensus for its clinical application [44, 45].

Despite the encouraging results of PBM therapy, this study had limitations associated with any preclinical study, considering that there are different levels of BMD resulting from various diseases that affect human bone metabolism. However, this means that the design of randomized clinical trials with the use of IRL will be interesting because it does not have any side effects.

Conclusion

Based on the study findings, it can be concluded that IRL in a single application increased new bone formation and favored bone dynamism mainly in the OVX/IR group. Owing to the encouraging results, future clinical studies using IRL are fundamental, including in patients with bone metabolism deficits, in search of application protocols to achieve a clinical consensus.

Author contribution All authors have made substantial contributions to all of the following: (1) the conception and design of the study, or acquisition of data, or analysis and interpretation of data, (2) drafting the article or revising it critically for important intellectual content, (3) final approval of the version to be submitted. Additionally, all authors have read and concur with the content in the manuscript.

Funding Acknowledgements to Fundação de Amparo a Pesquisa do Estado de São Paulo—FAPESP (Award Numbers: 2018/11496-0; 2016/20297-6), for the indispensable subsidy for this work to be carried out with excellence, contributing to the acquisition of all material of consumption necessary for this work.

Declarations

Conflict of interest The authors declare no competing interests.

References

1. Compston J (2010) Osteoporosis: social and economic impact. Radiol Clin North Am 48:477–482. https://doi.org/10.1016/J.RCL.2010.02.010
2. Teófilo JM, Azevedo ACB, Petenusci SO et al (2003) Comparison between two experimental protocols to promote osteoporosis in the maxilla and proximal tibia of female rats. Pesqui Odontol Bras 17:302–306. https://doi.org/10.1590/S1517-74912003000400002
3. Teófilo JM, Brentegani LG, Lamano-Carvalho TL (2004) Bone healing in osteoporotic female rats following intra-alveolar grafting of bioactive glass. Arch Oral Biol 49:755–762. https://doi.org/10.1016/J.ARCHORALBIO.2004.02.013
4. Glösel B, Kuchler U, Watzek G, Gruber R (2010) Review of dental implant rat research models simulating osteoporosis or diabetes. Int J Oral Maxillofac Implants 25:516–24
5. Thorngren KG, Norrman PO, Hommel A et al (2005) Influence of age, sex, fracture type and pre-fracture living on rehabilitation pattern after hip fracture in the elderly. Disabil Rehabil 27:1091–1097. https://doi.org/10.1080/09638280500056402
6. Schindl A, Schindl M, Pernerstorfer-Schön H, Schindl L (2000) Low-intensity laser therapy: a review. J Investig Med 48:312–326
7. Karu TI (1987) Special issue papers. Photobiological fundamentals of low-power laser therapy. IEEE J Quantum Electron 23:1703–1717. https://doi.org/10.1109/JQE.1987.1073236
8. Pinheiro ALB, Martinez Gerbi ME, de Assis LF et al (2009) Bone repair following bone grafting hydroxyapatite guided bone regeneration and infra-red laser photobiomodulation: a histological study in a rodent model. Lasers Med Sci 24:234–240. https://doi.org/10.1007/S10103-008-0556-0
9. Nascimento SB, Cardoso CA, Ribeiro TP et al (2010) Effect of low-level laser therapy and calcitonin on bone repair in castrated rats: a densitometric study. Photomed Laser Surg 28:45–49. https://doi.org/10.1089/PHO.2008.2396
10. Lopes CB, Pinheiro ALB, Sathaiah S et al (2007) Infrared laser photobiomodulation (lambda 830 nm) on bone tissue around dental implants: a Raman spectroscopy and scanning electronic microscopy study in rabbits. Photomed Laser Surg 25:96–101. https://doi.org/10.1089/PHO.2006.2030
11. Freitas IGF, Baranauskas V, Cruz-Höfling MA (2000) Laser effects on osteogenesis. Appl Surf Sci 154:548–554. https://doi.org/10.1016/S0169-4332(99)00431-6
12. Abd-Elaal AZ, El-Mekawii HA, Saafan AM et al (2015) Evaluation of the effect of low-level diode laser therapy applied during the bone consolidation period following mandibular distraction osteogenesis in the human. Int J Oral Maxillofac Surg 44:989–997. https://doi.org/10.1016/J.IJOM.2015.04.010
13. Chang WD, Wu JH, Wang HJ, Jiang JA (2014) Therapeutic outcomes of low-level laser therapy for closed bone fracture in the human wrist and hand. Photomed Laser Surg 32:212–218. https://doi.org/10.1089/PHO.2012.3398
14. Nesioonpour S, Mokmeli S, Vojdani S et al (2014) The effect of low-level laser on postoperative pain after tibial fracture surgery: a double-blind controlled randomized clinical trial. Anesth Pain Med 4:e17350. https://doi.org/10.5812/AAPM.17350
15. Bayat M, Virdi A, Jalalifirouzkouhi R, Rezaei F (2018) Comparison of effects of LLLT and LIPUS on fracture healing in animal models and patients: a systematic review. Prog Biophys Mol Biol 132:3–22. https://doi.org/10.1016/J.PBIOMOLBIO.2017.07.004
16. Briteño-Vázquez M, Santillán-Díaz G, González-Pérez M et al (2015) Low power laser stimulation of the bone consolidation in tibial fractures of rats: a radiologic and histopathological analysis. Lasers Med Sci 30:333–338. https://doi.org/10.1007/S10103-014-1673-6
17. Sella VRG, do Bomfim FRC, Machado PCD et al (2015) Effect of low-level laser therapy on bone repair: a randomized controlled experimental study. Lasers Med Sci 30:1061–1068. https://doi.org/10.1007/S10103-015-1710-0
18. Polo TOB, Momesso GAC, Silva WPP et al (2021) Is an anodizing coating associated to the photobiomodulation able to optimize bone healing in ovariectomized animal model? J Photochem Photobiol B 217:112167. https://doi.org/10.1016/J.JPHOTOBIOL.2021.112167
19. Evans HM, Long JA (1922) Characteristic effects upon growth, oestrus and ovulation induced by the intraperitoneal administration of fresh anterior hypophyseal substance. Proc Natl Acad Sci U S A 8:38–39. https://doi.org/10.1073/PNAS.8.3.38
20. Luvizuto ER, Dias SMD, Queiroz TP et al (2010) Osteocalcin immunolabeling during the alveolar healing process in ovariectomized rats treated with estrogen or raloxifene. Bone 46:1021–1029. https://doi.org/10.1016/J.BONE.2009.12.016
21. Ramalho-Ferreira G, Faverani LP, Grossi-Oliveira GA et al (2015) Alveolar bone dynamics in osteoporotic rats treated with raloxifene or alendronate: confocal microscopy analysis. J Biomed Opt 20:038003. https://doi.org/10.1117/1.JBO.20.3.038003
22. Luvizuto ER, Queiroz TP, Dias SMD et al (2010) Histomorphometric analysis and immunolocalization of RANKL and OPG during the alveolar healing process in female ovariectomized rats treated with oestrogen or raloxifene. Arch Oral Biol 55:52–59. https://doi.org/10.1016/J.ARCHORALBIO.2009.11.001
23. Ramalho-Ferreira G, Faverani LP, Momesso GAC et al (2017) Effect of antiresorptive drugs in the alveolar bone healing. A histometric and immunohistochemical study in ovariectomized rats. Clin Oral Investig 21:1485–1494. https://doi.org/10.1007/S00784-016-1909-X
24. Momesso GAC, Polo TOB, da Silva WPP et al (2021) Miniplates coated by plasma electrolytic oxidation improve bone healing of simulated femoral fractures on low bone mineral density rats. Mater Sci Eng C Mater Biol Appl 120:111775. https://doi.org/10.1016/J.MSEC.2020.111775
25. Polo TOB, da Silva WP, Momesso GAC et al (2020) Plasma electrolytic oxidation as a feasible surface treatment for biomedical applications: an in vivo study. Sci Rep 10:10000. https://doi.org/10.1038/S41598-020-65289-2
26. Momesso GAC, de Souza Santos AM, Fonsecae Santos JM et al (2020) Comparison between plasma electrolytic oxidation coating and sandblasted acid-etched surface treatment: histometric, tomographic, and expression levels of osteoclastogenic factors in osteoporotic rats. Materials (Basel) 13:1–15. https://doi.org/10.3390/MA13071604
27. Faverani LP, Polo TOB, Ramalho-Ferreira G et al (2018) Raloxifene but not alendronate can compensate the impaired osseointegration in osteoporotic rats. Clin Oral Investig 22:255–265. https://doi.org/10.1007/S00784-017-2106-2
28. Thormann U, el Khawassna T, Ray S et al (2014) Differences of bone healing in metaphyseal defect fractures between osteoporotic and physiological bone in rats. Injury 45:487–493. https://doi.org/10.1016/J.INJURY.2013.10.033
29. Alt V, Thormann U, Ray S et al (2013) A new metaphyseal bone defect model in osteoporotic rats to study biomaterials for the enhancement of bone healing in osteoporotic fractures. Acta Biomater 9:7035–7042. https://doi.org/10.1016/J.ACTBIO.2013.02.002

30. Bouxsein ML, Boyd SK, Christiansen BA et al (2010) Guidelines for assessment of bone microstructure in rodents using micro-computed tomography. J Bone Miner Res 25:1468–1486. https://doi.org/10.1002/JBMR.141
31. Thompson DD, Simmons HA, Pirie CM, Ke HZ (1995) FDA Guidelines and animal models for osteoporosis. Bone 17:S125–S133. https://doi.org/10.1016/8756-3282(95)00285-L
32. Oliver RA, Yu Y, Yee G et al (2013) Poor histological healing of a femoral fracture following 12 months of oestrogen deficiency in rats. Osteoporos Int 24:2581–2589. https://doi.org/10.1007/S00198-013-2345-2
33. Namkung-Matthai H, Appleyard R, Jansen J et al (2001) Osteoporosis influences the early period of fracture healing in a rat osteoporotic model. Bone 28:80–86. https://doi.org/10.1016/S8756-3282(00)00414-2
34. Campenfeldt P, Al-Ani A, Hedström M, Ekström W (2018) Low BMD and high alcohol consumption predict a major re-operation in patients younger than 70 years of age with a displaced femoral neck fracture-a two -year follow up study in 120 patients. Injury 49:2042–2046. https://doi.org/10.1016/J.INJURY.2018.09.025
35. KazemShakouri S, Soleimanpour J, Salekzamani Y, Oskuie MR (2010) Effect of low-level laser therapy on the fracture healing process. Lasers Med Sci 25:73–77. https://doi.org/10.1007/S10103-009-0670-7
36. RajaeiJafarabadi M, Rouhi G, Kaka G et al (2016) The effects of photobiomodulation and low-amplitude high-frequency vibration on bone healing process: a comparative study. Lasers Med Sci 31:1827–1836. https://doi.org/10.1007/S10103-016-2058-9
37. Pinheiro ALB, Soares LGP, da Silva ACP et al (2020) Raman spectroscopic study of the effect of the use of laser/LED phototherapy on the repair of complete tibial fracture treated with internal rigid fixation. Photodiagnosis Photodyn Ther 30:101773. https://doi.org/10.1016/J.PDPDT.2020.101773
38. Pretel H, Lizarelli RFZ, Ramalho LTO (2007) Effect of low-level laser therapy on bone repair: histological study in rats. Lasers Surg Med 39:788–796. https://doi.org/10.1002/LSM.20585
39. Nicolau RA, Jorgetti V, Rigau J et al (2003) Effect of low-power GaAlAs laser (660 nm) on bone structure and cell activity: an experimental animal study. Lasers Med Sci 18:89–94. https://doi.org/10.1007/S10103-003-0260-Z
40. Hamblin MR (2017) Mechanisms and applications of the anti-inflammatory effects of photobiomodulation. AIMS Biophys 4:337–361. https://doi.org/10.3934/BIOPHY.2017.3.337
41. Tsai SR, Hamblin MR (2017) Biological effects and medical applications of infrared radiation. J Photochem Photobiol B 170:197–207. https://doi.org/10.1016/J.JPHOTOBIOL.2017.04.014
42. Amaroli A, Colombo E, Zekiy A et al (2020) Interaction between laser light and osteoblasts: photobiomodulation as a trend in the management of socket bone preservation-a review. Biology (Basel) 9:1–15. https://doi.org/10.3390/BIOLOGY9110409
43. Wan Z, Zhang P, Lv L, Zhou Y (2020) NIR light-assisted phototherapies for bone-related diseases and bone tissue regeneration: a systematic review. Theranostics 10:11837–11861. https://doi.org/10.7150/THNO.49784
44. Mohsenifar Z, Fridoni M, Ghatrehsamani M et al (2016) Evaluation of the effects of pulsed wave LLLT on tibial diaphysis in two rat models of experimental osteoporosis, as examined by stereological and real-time PCR gene expression analyses. Lasers Med Sci 31:721–732. https://doi.org/10.1007/S10103-016-1916-9
45. Fridoni M, MasteriFarahani R, Nejati H et al (2015) Evaluation of the effects of LLLT on biomechanical properties of tibial diaphysis in two rat models of experimental osteoporosis by a three point bending test. Lasers Med Sci 30:1117–1125. https://doi.org/10.1007/S10103-014-1706-1